

Competition between Hydrogen Bonds and Lewis Acid-Base Interactions in the Equilibria between Bis(pentafluorophenyl)borinic Acid and Pyridine: Insights from NMR, Diffractometric and Computational Studies

By Daniela Maggioni, Tiziana Beringhelli, Giuseppe D'Alfonso,
Maria Carlotta Malatesta, Pierluigi Mercandelli*, and Daniela Donghi*[#]

Dipartimento di Chimica, Università degli Studi di Milano, via Golgi 19, 20133 Milano, Italy

Dedicated to Prof. Dr. Hans-Heinrich Limbach on the occasion of his 70th birthday

(Received December 17, 2012; accepted February 26, 2013)

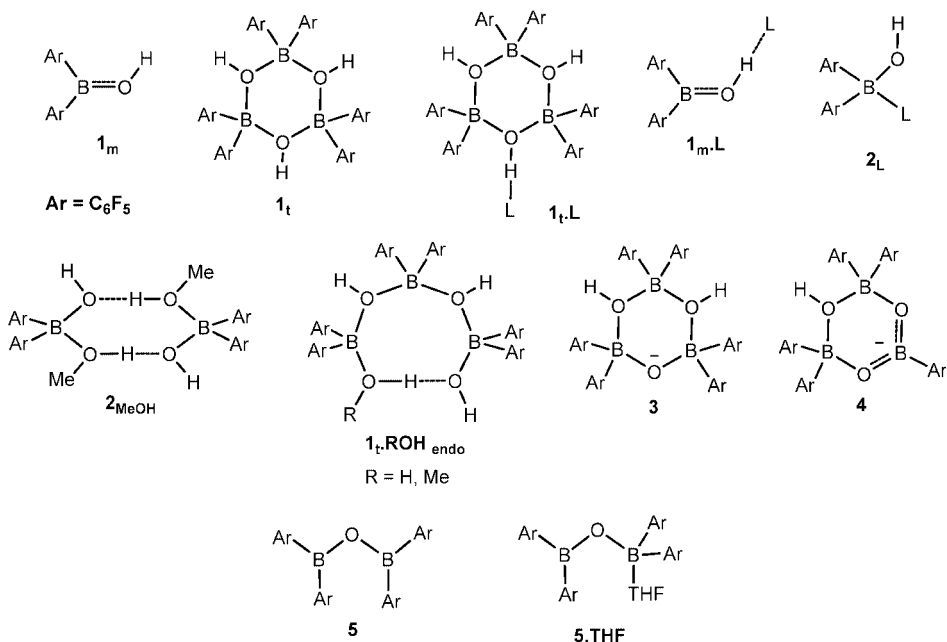
(Published online June 10, 2013)

Hydrogen Bond / Lewis Bases / ¹⁹F NMR Spectroscopy / DFT Computations / Fluoroarylboranes

¹H and ¹⁹F NMR spectroscopy, X-ray diffractometry and DFT computations have been used for investigating the interaction between the Lewis base pyridine and bis(pentafluorophenyl)borinic acid Ar₂BOH (**1**, Ar = C₆F₅). Previous studies showed that the latter species in solution exists as an equilibrium mixture of the monomer (**1_m**) and a cyclic trimer (**1_t**), in variable ratios, and that the trimer is stabilized in the presence of Lewis bases, by the formation of strong **1_t**⋯**L** hydrogen bonds. In the present case, upon addition of 0.33 equivalents of pyridine, low-temperature NMR spectra showed the formation of deprotonated **1_t** (anion **3**), strongly hydrogen-bonded to the pyridinium cation Hpy⁺. The presence of this cation was confirmed by the high value of ¹J_{HN} (88 Hz). DFT computations confirmed the higher stability of the O⁻⋯H–N⁺ limit form over the neutral O–H⋯N one. Variable temperature NMR spectra showed that the Hpy⁺⋯**3** ion pair has high conformational freedom. At temperatures higher than 260 K, **3** underwent reversible partial fragmentation to give **1_m** and the Lewis acid-base covalent adducts between pyridine and either **1_m** (**2_{py}**), or its anhydride (**5_{py}**). The fragmentation was perfectly reversible on lowering the temperature. The adduct **2_{py}** became the only species in solution in the presence of 1 equivalent of pyridine, showing that the Lewis basicity of pyridine plays the major role, at variance with what previously observed with other bases. Hydrogen bond interactions, however, promote the supramolecular organization of **2_{py}** in the form of a cyclic tetramer, as revealed by X-ray single crystal diffractometric analysis. The formation of the deprotonated trimer **3** was previously observed in the reaction of **1** with 1,8-bis(dimethylamino)naphthalene (DMAN). However

* Corresponding authors. E-mail: daniela.donghi@aci.uzh.ch; pierluigi.mercandelli@unimi.it

[#] Present address: Institute of Inorganic Chemistry, University of Zurich, Winterthurerstrasse 190, CH-8057 Zurich, Switzerland



Scheme 1. The main species previously observed in dichloromethane solutions of Ar_2BOH (**1**, $\text{Ar} = \text{C}_6\text{F}_5$), alone or in the presence of bases L , with $\text{L} =$ water, tetrahydrofuran (THF), methanol (MeOH) or 1,8-bis(dimethylamino)naphthalene (DMAN).

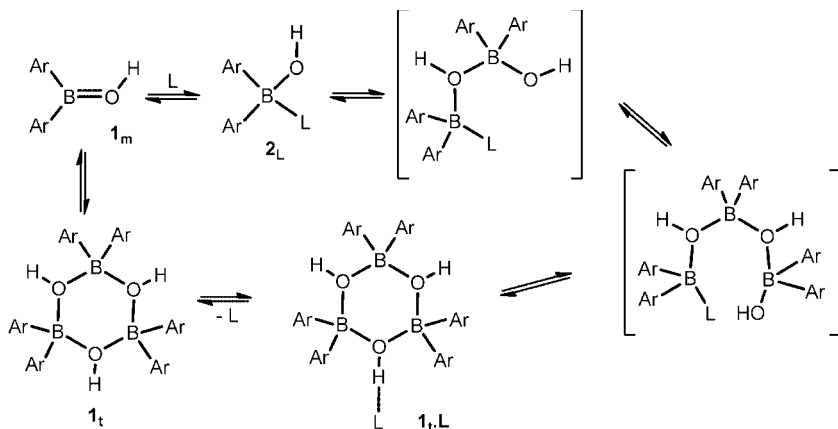
the stepwise dearylation processes, which were dominant in the reactions with DMAN, have a very marginal role in the reaction with pyridine, due to its lower Brønsted basicity.

For Supplementary Material see online version. Supporting information available: details of the NMR spectroscopic characterization (Figs. S1–S4), computed chemical shifts (Table S1), details of the X-ray diffractometric analysis, and tables of geometrical parameters (Tables S2–S3).

1. Introduction

Bis(pentafluorophenyl)boronic acid Ar_2BOH (**1**, $\text{Ar} = \text{C}_6\text{F}_5$), is an intriguing Lewis acid, which is able to dramatically modify its speciation in solution in response to external stimuli [1]. These properties have stimulated a number of fundamental investigations [2–7], as well as applications in synthesis and catalysis [8,9].

The chameleonic nature of this small molecule arises from a peculiar combination of properties of opposite sign: Lewis and Brønsted acid and base, hydrogen bond donor and acceptor. The Lewis acidity of boron and the Lewis basicity of oxygen, although depressed by the partial double-bond character of the boron-oxygen interaction [2], are strong enough to promote the auto-association equilibrium (**1**). Therefore solutions of **1** always contain both the monomeric (**1_m**) and the trimeric (**1_t**) forms depicted in Scheme 1, in a ratio which depends on temperature, concentration and polarity of the solvent [3]. The monomer is usually largely dominant, while in the solid state the trimer



Scheme 2. Trimerization pathway in the presence of L , as suggested by DFT computations [3]. In square brackets are indicated intermediates undetected in our experimental conditions.

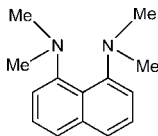
only is present [2].



Interestingly, position and rate of equilibrium 1 are strongly affected by the presence of even small amounts of Lewis bases L , like tetrahydrofuran (THF) [4] or H_2O [3]. In general, in the absence of base, equilibrium (1) is slow and $\mathbf{1}$ is mainly in its monomeric form. Nevertheless, the presence of water accelerates the equilibrium [3], and instantaneous complete trimerization was observed at 173 K upon addition of stoichiometric THF to dichloromethane solutions of $\mathbf{1}$ (0.33 equivalents of L with respect to the Ar_2BOH units) [4]. DFT computations showed that the presence of L is responsible for the aggregation pathway depicted on the right side of Scheme 2 [3]. The kinetic barriers of such pathway are lower than in the absence of L , and this explains the acceleration effect of L in the aggregation process. The shift to the right of the equilibrium arises from the high stability of the hydrogen-bonded trimeric species $\mathbf{1}_t \cdot \text{L}$. The formation of this species is preferred to that of the Lewis acid-base adduct $\mathbf{2}_L$, highlighting the low Lewis acidity of the boron atom in $\mathbf{1}_m$.

In principle, a Lewis base has two potential way of interaction with $\mathbf{1}_m$: *via* covalent bond with the boron atom or *via* hydrogen bond with the BOH group. This results in a complex interplay between hydrogen bonding and Lewis acid-base interactions, well evidenced by the different preferred way of interacting with $\mathbf{1}_m$ shown by H_2O and THF. In the first case, covalent Lewis acid-base interaction was preferred, leading to the formation of adduct $\mathbf{2}_L$, with a tetra-coordinated boron atom, whereas in the case of THF the interaction occurred *via* hydrogen bond ($\mathbf{1}_m \cdot \text{L}$ in Scheme 1), leaving tri-coordinated the boron atom.

For Lewis bases able to act also as hydrogen bond donors, such as H_2O or methanol (MeOH) it was found that the two functionalities can work in a cooperative way, affording very stable species in which the bases are simultaneously B-bonded and H-bonded.



Scheme 3. 1,8-Bis(dimethylamino)naphthalene (DMAN).

This is the case of the trimeric adducts containing one endocyclic hydrogen-bonded water/methanol molecule, $\mathbf{1}_t \cdot \text{ROH}_{\text{endo}}$ shown in Scheme 1. The stabilization of the water molecule in this environment was so strong to promote water formation, by spontaneous partial dehydration of borinic acid to its anhydride (**5** in Scheme 1). In the case of methanol, the formation of such species, in the presence of 0.33 equivalents of MeOH, occurred preferentially with respect to the formation of the $\mathbf{1}_t \cdot \text{MeOH}$ adduct. The same twofold interaction allowed stabilization by dimerization of the adduct $\mathbf{2}_{\text{MeOH}}$ (shown in Scheme 1), thus inhibiting the fast trimerization pathway operative with THF and H_2O .

A fully different behaviour was observed in the presence of the Brønsted base 1,8-bis(dimethylamino)naphthalene (DMAN, Scheme 3) [6]. In this case, the strongest accelerating effect in the $\mathbf{1}_m$ - $\mathbf{1}_t$ equilibrium was observed, since catalytic amounts of base promoted the complete conversion of $\mathbf{1}_m$ into $\mathbf{1}_t$. This trimerization reaction most likely occurs *via* a pathway that includes first deprotonation of $\mathbf{1}_m$, with consequent formation of deprotonated $\mathbf{1}_t$ (**3** in Scheme 1). In addition to deprotonation, fast irreversible dearylation reactions took place, leading to the formation of the penta-aryl and tetra-aryl boroxinate anions $\text{Ar}_5\text{B}_3(\text{OH})\text{O}_2^-$ (**4** in Scheme 1) and $\text{Ar}_4\text{B}_3\text{O}_3^-$. Base catalyzed hydrolysis of $\mathbf{1}_m$ to its boronate analogue $\text{ArB}(\text{OH})\text{O}^-$, followed by aggregation and condensation, is the most likely mechanism leading to the first dearylation process, which occurs in parallel to the formation of the deprotonated trimer **3** of Scheme 1 [6].

Taken together, all the previous evidence allowed depicting an elaborate but still not comprehensive picture of the possible interactions between **1** and various bases. Changing only slightly the characteristics of the interacting base could give rise to unexpected behaviours. It was therefore of interest to investigate how the title compound reacts in the presence of a molecule like pyridine. This molecule is able to act both as a Brønsted and as a Lewis base, as well as a hydrogen bond acceptor, but, unlike water and methanol, it does not have any hydrogen-bond donor ability. The study was addressed both spectroscopically, by use of variable temperature ^1H and ^{19}F NMR spectra, and theoretically, by using DFT computations.

2. Experimental

All manipulations were performed under inert atmosphere (N_2 or Ar) using oven dried Schlenk-type glassware. CD_2Cl_2 (C.I.L.) was anhydri-fied over activated molecular sieves. Ar_2BOH was a gift from Basell Polyolefins. Deuterated pyridine (py- d_5 , D 100%) was purchased by Aldrich and used as received. All the NMR spectra were acquired with a Bruker AVANCE DRX-300 spectrometer, equipped with a 5-mm TBI probe or with a 5-mm QNP probe, with a Bruker AVANCE DRX-400 spectrometer,

equipped with a 5-mm BBI probe, and with a Bruker AC-200 spectrometer, equipped with a 5 mm BBI probe. ¹⁹F NMR spectra were referenced to external CFCl₃. ¹¹B NMR spectra were referenced to external BF₃·Et₂O. Pentafluorotoluene (C₆F₅CH₃, 1 μL) was added as internal standard (std) for both ¹H and ¹⁹F NMR spectra. The temperature was calibrated with a standard CH₃OH/CD₃OD solution [10].

2.1 Sample preparation and NMR experiments

Different amounts of **1** were weighted directly into the NMR tube under N₂ and dissolved in measured amounts of pre-dried CD₂Cl₂, affording typically *ca.* 0.1 M solutions. Stepwise additions of pyridine with a micro syringe were done directly into the NMR tube, both at low and at room temperature. No significant differences in the spectra were observed in the two cases. The experiments were usually carried on using pyridine-d₅, to avoid the overlap of the aromatic signals of pyridine with the signals of the B–OH groups in the proton spectra.

After each addition, ¹H and ¹⁹F NMR spectra were recorded. Variable temperature mono and bidimensional experiments were performed on samples containing *ca.* 0.33 equivalents (hereafter equiv) of pyridine in the range 173–293 K. These experiments were useful to evaluate the speciation of **1** at different temperatures, as well as to evaluate the inter- and intra-molecular dynamic processes undergone by the various species in solution. [¹⁹F,¹⁹F]-EXSY experiments recorded at different temperatures confirmed the nature of the observed exchange processes, as discussed in the text. In addition, a [¹H,¹⁹F]-HOESY experiment recorded at low temperature suggested the presence of hydrogen-bond interactions between the OH resonances and the *ortho* fluorine of the aryl rings. A ¹¹B NMR spectrum was recorded at 293 K to confirm the ratio between species containing tetra- and tri-coordinated boron atoms.

The titration with py-d₅ was carried on up to 1 equiv, and the corresponding spectra (¹H, ¹⁹F and ¹¹B) recorded at different temperatures.

A sample in which 0.33 equiv of ¹⁵N-pyridine (purchased by C.I.L., ¹⁵N 98%) were added to **1** was also prepared, and ¹H NMR spectra at low temperature were recorded to confirm the presence of pyridinium cation (see below).

2.2 Computational details

Ground state geometries were optimized by means of density functional calculations employing the hybrid functional B3LYP [11] along with the standard valence double- ζ polarized basis set 6-31G(d,p). All the calculations were done without imposing any symmetry, however the species **1**, **py** and Hpy⁺·**3** resulted to possess C₂ symmetry. The nature of all the stationary points was checked by computing vibrational frequencies and all the species were found to be true minima. Single point energy calculations were done in presence of solvent (dichloromethane, used in the NMR studies) described by the polarizable continuum model (PCM) by means of the integral equation formalism variant [12]. NMR shielding tensors were computed with the gauge-independent atomic orbital (GIAO) method [13] at the B3LYP/6-31++G(d,p) level of theory [14].

Chemical shift are referenced to TMS and CFCl_3 for ^1H and ^{19}F , respectively. All the calculations were done with Gaussian 09 [15].

2.3 X-ray diffractometric analysis

Colorless crystals of $\text{Ar}_2\text{B}(\text{OH})(\text{py})$ ($\mathbf{2}_{\text{py}}$) were obtained by slow diffusion of *n*-pentane into a dichloromethane solution of a 1 : 1 Ar_2BOH /pyridine mixture, at 248 K. Crystal data: $\text{C}_{17}\text{H}_6\text{BF}_{10}\text{NO}$, $M_r = 441.04$, triclinic, space group $P\bar{1}$ (No. 2), $a = 14.166(2)$ Å, $b = 14.833(2)$ Å, $c = 16.752(2)$ Å, $\alpha = 83.81(2)^\circ$, $\beta = 77.80(2)^\circ$, $\gamma = 85.63(2)^\circ$, $V = 3415.3(8)$ Å³, $Z = 8$, $d_{\text{calc}} = 1.715$ g cm⁻³, $T = 295(2)$ K, crystal size = $0.28 \times 0.28 \times 0.16$ mm, $\mu = 0.18$ mm⁻¹, $\lambda = 0.71073$ Å (Mo $K\alpha$). Refinement of 1085 parameters on 12081 independent reflections out of 38 878 measured reflections ($R_{\text{int}} = 0.0465$, $R_\sigma = 0.0369$, $2\theta_{\text{max}} = 50.1^\circ$) led to $R_1 = 0.0397$ ($I > 2\sigma(I)$), $wR_2 = 0.1185$ (all data), and $S = 1.065$, with the largest peak and hole of 0.238 and -0.207 e Å⁻³. Details of the diffractometric analysis can be found in the Supporting Information. CCDC-915451 contains the crystallographic data for $\mathbf{2}_{\text{py}}$. These data can be obtained free of charge from The Cambridge Crystallographic Data Centre.

3. Results and discussion

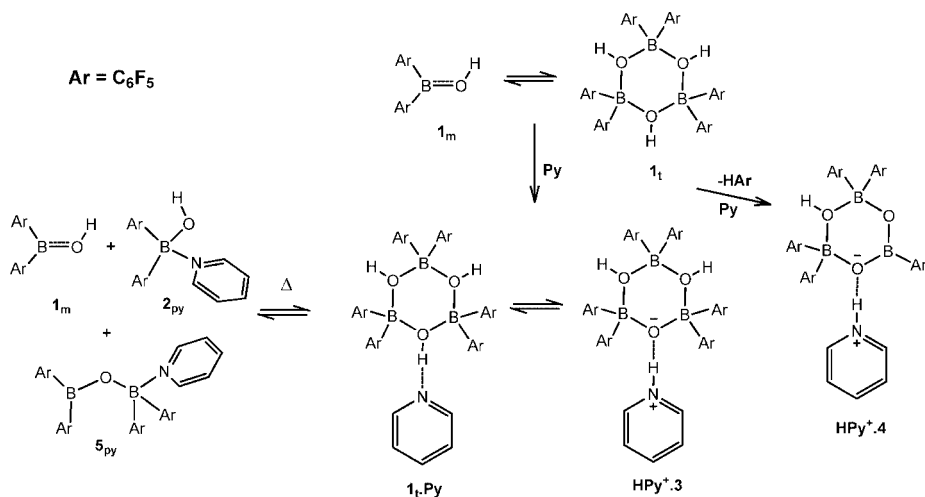
3.1 The reaction of **1** with 0.33 equivalents of pyridine at low temperature

The ^1H and ^{19}F NMR spectra showed that the addition, at 178 K, of *ca.* 0.33 equiv of pyridine (with respect to the moles of Ar_2BOH present in solution) caused the complete disappearance of the starting compound, accompanied by the formation of two trimeric species.

The main reaction product (accounting for *ca.* 80–90% of the species in solution) can be formulated as the ion pair between deprotonated $\mathbf{1}_t$ and the pyridinium cation ($\text{Hpy}^+ \cdot \text{Ar}_6\text{B}_3(\text{OH})_2\text{O}^-$, *i.e.* $\text{Hpy}^+ \cdot \mathbf{3}$, depicted in Scheme 4), on the base of the following evidence. The trimeric structure agrees both with the chemistry (0.33 equiv of pyridine) and with the NMR data. The ^{19}F spectrum (Fig. 1), although heavily affected by various dynamic processes not completely frozen even at very low temperatures (see Sect. 3.3), at 173 K showed three signals with the same integrated intensity in the *para* region of the spectrum (see inset of Fig. 1), two of which were broad and rapidly coalesced on raising the temperature. At 293 K, the ^{19}F spectrum shows two sets of signals in 1 : 2 ratio in the *ortho* and *para* regions, whereas only one signal is present in the *meta* region due to accidental overlap. The attributions of these signals to a single species were confirmed by a [^{19}F , ^{19}F]-COSY experiment (Fig. S1 in Supporting Information).

The ^1H spectrum at 178 K showed two resonances in the 1 : 2 ratio, at δ 17.01 and 7.86, respectively. The position of the lower field resonance indicates that one proton is involved in a strong $\text{O} \cdots \text{H} \cdots \text{N}$ hydrogen bond. The value of the chemical shift cannot discriminate between the neutral $\text{O}-\text{H} \cdots \text{N}$ or charged $\text{O}^- \cdots \text{H}-\text{N}^+$ limit forms, *i.e.* cannot establish if proton transfer (Eq. 2) to the N atom of the Brønsted base pyridine (with pyridinium formation) occurred or not.





Scheme 4. A summary of the equilibria operative in solutions of **1** upon pyridine addition.

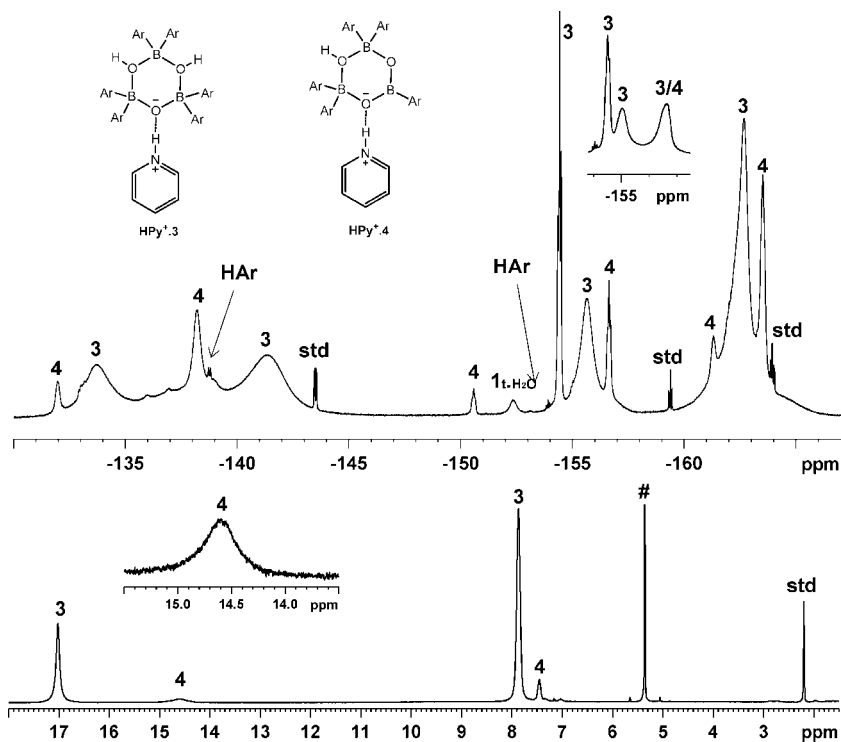


Fig. 1. ^{19}F NMR (top, 178 K, inset at 173 K, 9.4T) and 1H NMR (bottom, 178 K) spectra of **1** treated with *ca.* 0.33 equiv of $py-d_5$ (7.1T; std is pentafluorotoluene, used as internal standard; HAr is C_6F_5H ; # indicates the signal due to the CD_2Cl_2 solvent). $1_t \cdot H_2O$ indicates the small amount of the adduct between **1**_t and water [3] arising from adventitious water present in the solution.

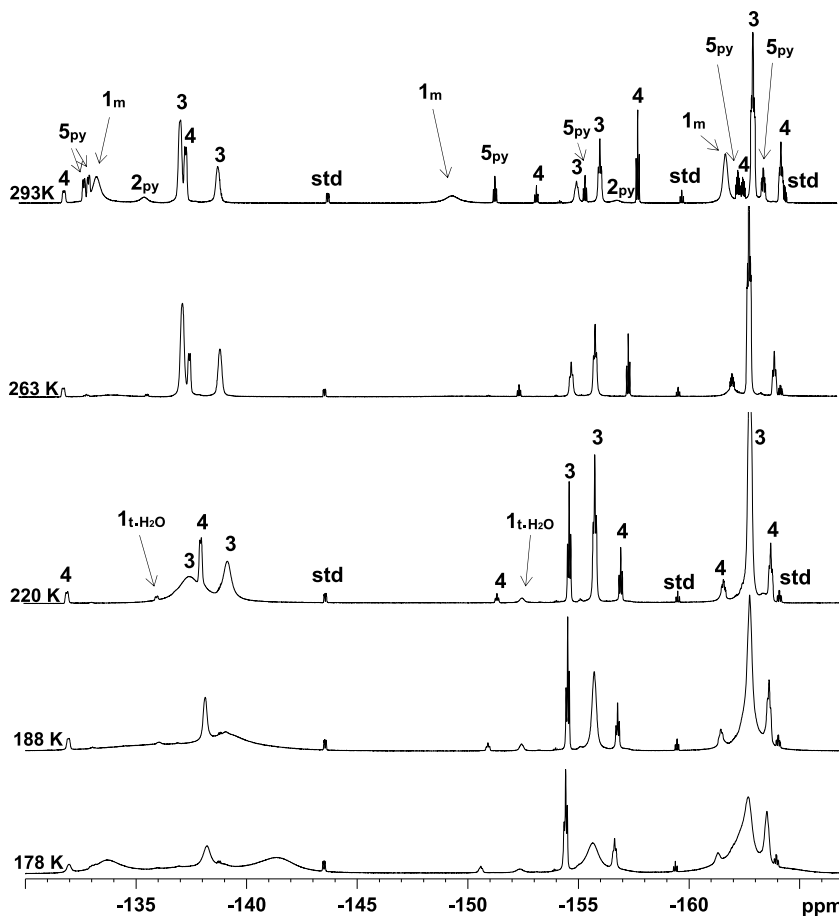


Fig. 2. Variable temperature ^{19}F NMR spectra of a sample of **1** treated with *ca.* 0.33 equiv of py-d_5 (CD_2Cl_2 , 7.1T). $\mathbf{1_t \cdot H_2O}$ indicates the adduct between $\mathbf{1_t}$ and water [3].

For this reason an experiment with $^{15}\text{NC}_5\text{H}_5$ was performed: in this case the NH resonance of **3** (as well as that of **4**, described below), appeared as a doublet with $J_{\text{HN}} = 88$ Hz. Such a high value of J_{HN} is typical of the pyridinium cation [16], so definitely confirming the ionic nature of the species present in solution at low temperature. The signal remained a sharp doublet up to 283 K, then broadened, as the result of the several intermolecular exchange processes occurring at room temperature. DFT computations support the formulation of the adduct as a double-charged hydrogen-bonded species. Indeed, even if a geometry optimization of $\text{Hpy}^+ \cdot \mathbf{3}$ and $\mathbf{1_t} \cdot \text{py}$ shows that both the species correspond to minima of C_2 symmetry, differing almost exclusively in the position of the hydrogen atom involved in the hydrogen bond [17], the neutral species is computed to lie 17 kJ mol^{-1} higher in energy than the charged one.

A second product, accounting for *ca.* 10% of species in solution, was identified as the ion pair $\text{Hpy}^+ \cdot \mathbf{4}$ (see Scheme 4). This species is responsible for two resonances

in the ratio 1 : 1 in the ¹H spectrum (one, sharp, at δ 7.45 ppm and another, broad, at δ 14.60, the latter being attributable to a hydrogen-bonded proton) and for two resonances in the ratio 1 : 4 in each of the *ortho*, *para* and *meta* regions of the ¹⁹F spectra. Such C_{2v} pattern of the ¹⁹F signals, which is typical of pentaarylboroxinates, indicates easy migration of the hydrogen-bonded pyridinium cation between the two deprotonated oxygen atoms. A similar pattern was observed for the ion pair HDMAN⁺·**4** [6]. The three sets of 1 : 4 resonances are clearly detected at temperatures higher than 180 K (see Fig. 2), whereas at lower temperatures partial overlaps occurred with the broad and more intense ¹⁹F signals of the major product **3** (Fig. 1). Their attribution to a unique species was confirmed by the [¹⁹F, ¹⁹F]-COSY experiment recorded at 293 K (Fig. S1 in Supporting Information). The comparison between the ¹H and ¹⁹F intensity ratios (by use of pentafluorotoluene as internal standard in both the spectra) confirmed that the most intense signal in each of the *ortho*, *para* and *meta* regions was due to four equivalent aryl rings. Further support to the formulation of this species was provided by the separation between the *meta* and *para* ¹⁹F signals ($\Delta\delta_{m,p}$). At low temperature $\Delta\delta_{m,p}$ of 10.8 and 6.9 ppm were found for the signals of intensity 1 and 4, respectively. This is in line with previous findings, that showed that $\Delta\delta_{m,p}$ is smaller for tetra-coordinated than for tri-coordinated boron compounds, due to the stronger upfield shift of the ¹⁹F *para* resonances resulting from the increased electron density on the tetra-coordinated boron atom [1]. A similar pattern was observed for the ¹⁹F *para* and *meta* resonances of HDMAN⁺·**4** [6].

Even if the general behaviour is similar, the absolute values of ¹H and ¹⁹F NMR chemical shifts for the Hpy⁺·**3** and Hpy⁺·**4** ion pairs (see Table 1) were found to be quite different with respect to those of the analogous species identified in the reaction of **1** with DMAN (see for instance, for the *para* ¹⁹F resonances at 178 K: -154.3 and -155.6 ppm for Hpy⁺·**3** vs. -156.0 and -159.0 ppm for HDMAN⁺·**3**; see also -150.5 and -156.6 ppm for Hpy⁺·**4**, vs. -154.1 and -158.1 ppm for HDMAN⁺·**4**). These differences are attributable to the different nature (tight or loose) of the ion pairs in the two compounds, as discussed in the following Sect. 3.4. Such differences mainly affect the resonances of the aryl groups closer to the O⁻···Hpy⁺ site, *i.e.* the ones of higher intensity in **3** and the ones of lower intensity in **4**.

Two separated resonances are observed for the NH⁺ protons of the two ion pairs Hpy⁺·**3** and Hpy⁺·**4** (**3** δ 17.01, **4** δ 14.60), unlike what previously observed for HDMAN⁺·**3** and HDMAN⁺·**4**, where only one averaged signal for HDMAN⁺ was present, at δ 20.1 ppm. The large sterical hindrance of the HDMAN⁺ cation prevents any close interaction with **3** or **4**, resulting in an averaged signal, whose position is determined by the strength of the N···H···N⁺ intra-molecular hydrogen bond. In the present case, the two separated resonances for Hpy⁺·**3** and Hpy⁺·**4** agree with the presence of a hydrogen-bond interaction between anion and cation. In particular, the higher field value for the proton resonance of **4** suggests that in this species the hydrogen-bond interaction is weaker than in **3**. This is in line with the lower propensity of the deprotonated oxygen atoms of **4** to accept hydrogen bond, being involved in partial π -donation to the tri-coordinated boron atom [6] (as depicted in Scheme 1). Moreover, in **4** the negative charge is delocalized over the two equivalent oxygen atoms surrounding tri-coordinated boron, while in **3** it is localized on the unique deprotonated oxygen atom. Nevertheless, at 220 K the signals of the NH⁺ protons coalesced in an averaged signal

Table 1. ^1H and ^{19}F chemical shift of the pyridine derivatives described in this work (CD_2Cl_2).

	T [K]	$\delta^1\text{H}$ [ppm]			$\delta^{19}\text{F}$ [ppm]			$\Delta\delta_{m,p}$ [ppm]
		NH	OH	<i>ortho</i>	<i>para</i>	<i>meta</i>		
2_{py}	173		4.1	-135.5 (2)	-157.5 (1)	-163.7 (2)	6.2	
	293		4.4	-135.5 (2)	-157.0 (1)	-163.4 (2)	6.4	
3	178	17.01	7.86	-133.6 (4)	-154.3 (2)	-162.6 (12)	8.3, 7.0	
				-141.4 (8)	-155.6 (4)			
	170	17.00	7.87	-133.7 (4)	-154.2 (2)	-161.1 (2)		
				-136.7 (2)	-154.8 (2)	-162.1 (4)		
				-140.9 (2, $J_{\text{HF}} = 80$ Hz)	-156.3 (2)	-162.6 (2)		
			-142.0 (2)		-163.1 (2)			
			-142.1 (2, $J_{\text{HF}} = 80$ Hz)		-165.1 (2)			
4	178	14.60	7.45	-131.9 (2)	-150.5 (1)	-161.3 (2)	10.8	
				-138.1 (8)	-156.6 (4)	-163.5 (8)	6.9	
5_{py}	293			-132.9 (4)	-151.5 (2)	-162.4 (4)	11	
				-133.1 (4)	-155.6 (2)	-163.2 (4)	7.6	

at δ 16.70, (Fig. 3), indicating exchange of the Hpy^+ cation between anions **3** and **4** (see Sect. 3.2).

The formation of the pentaarylic anion **4** was never detected in the reaction of **1** with the Lewis bases THF, MeOH or H_2O , but only in the reaction with the Brønsted base DMAN [18]. In the latter case, however, after addition of 0.33 equiv at low temperature, the anions **3** and **4** were formed in comparable amounts, while with pyridine the amount of **4** hardly reached 10% of the products present in the mixture.

There is another significant difference between the behaviour of DMAN and pyridine. The latter does not play a catalytic role in the low-temperature trimerisation reaction, as it occurs with DMAN. The addition of less than 0.33 equiv of pyridine at 193 K does not cause complete trimerisation, as in the case of DMAN, but rather the increase of the trimeric species at expenses of **1_m**. From this point of view, the behaviour of **1** with pyridine is comparable to that observed with the Lewis base THF, where trimerization was complete only at 0.33 equiv of added base.

Moreover, at room temperature the conductivity of the solution obtained upon addition of 0.33 equiv of pyridine to **1** was very low (*ca.* 40 μS in CH_2Cl_2), much lower than in the case of the corresponding solution obtained with DMAN (*ca.* 500 μS , in the same conditions). This might result from two factors. The ion pairs involving Hpy^+ are expected to be much tighter and therefore much less conductor than those formed by HDMAN^+ , because in the latter case the proton is trapped by the two N atoms of the proton sponge cation and cannot establish a strong hydrogen bond interaction with the negative oxygen atom of **3** (see above). In addition, on increasing the temperature the $\text{O}^-\cdots\text{H}-\text{N}^+$ limit form of equilibrium **2** might progressively shifts towards the neutral $\text{O}-\text{H}\cdots\text{N}$ form, on the bases both of the thermodynamics of this kind of proton transfer equilibria [19] and of the decrease of the dielectric constant of CD_2Cl_2 at higher tem-

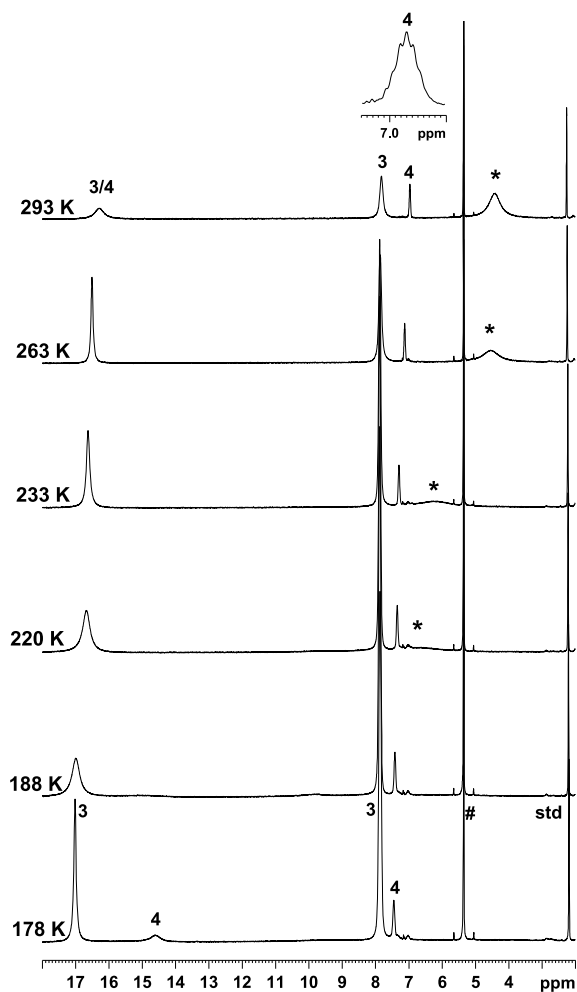


Fig. 3. Variable temperature 1H NMR spectra of a sample of **1** treated with *ca.* 0.33 equiv of $py-d_5$ (CD_2Cl_2 , 7.1T). The inset shows the fine structure of the BOH signal of **4**. The asterisk marks the average signal of **1_m**, **2_{H₂O}** and **2_{py}**. # marks the solvent signal.

perature [20]. The neutral form (corresponding to the **1₁**·**py** adduct) at high temperature undergoes fragmentation to the variety of neutral mono and dinuclear species described in the following paragraph.

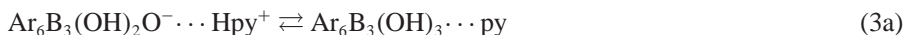
3.2 Partial fragmentation of $Hpy^+ \cdot 3$ at room temperature: the novel species **2_{py}** and **5_{py}**

On increasing the temperature the ^{19}F spectra dramatically changed (Fig. 2), as the result of the increase of the rate of the dynamic processes, which will be discussed in the next Sect. 3.3. Some of these processes involve fast dissociation/reaggregation of the

trimeric units. However, up to *ca.* 263 K such dissociative processes are kinetically but not thermodynamically significant, that means that the amount of the dissociation products is small, although sufficient to affect the exchange processes. On the contrary, at higher temperatures, the fragmentation increased, as revealed by the decrease of the intensity of the ^{19}F resonances of **3** (at 293 K they were reduced to about one half of their original intensity), and the appearance of the signals of **1_m** and of the new species **2_{py}** and **5_{py}**.

Species **2_{py}** contains one molecule of borinic acid (monomer) and one of pyridine. In these conditions it was in small concentration, and its resonances were barely detectable, being weak and broad, for intermolecular exchange. However its presence was unquestionably indicated by the cross peaks with **1_m** and **3** clearly recognizable in the [^{19}F , ^{19}F]-EXSY exchange spectrum shown in Fig. 4. Moreover, **2_{py}** became the main species in solution when the amount of pyridine exceeded 0.33 equiv (see Sect. 3.4 for details). It has been formulated as the Lewis acid-base adduct between **1_m** and pyridine, $\text{Ar}_2\text{B}(\text{OH})(\text{py})$ (**2_{py}** in Scheme 4), rather than the hydrogen-bonded species **1_m** ··· **py**, on the bases of many pieces of evidence. First, both its ^{11}B signal ($\delta 2.6$, Fig. S2 in Supporting Information) and the chemical shift difference between its ^{19}F *meta* and *para* resonances ($\Delta\delta_{m,p} = 6.4$ ppm) lie in the range typical for tetra-coordinated boron atoms. Second, DFT computations indicate a higher stability for this form with respect to the hydrogen-bonded one, by 7 kJ mol^{-1} . Finally, a X-ray analysis provided the details of its molecular and supramolecular structure (see Sect. 3.4).

The fragmentation process leading to **2_{py}** can therefore be described by equations 3, where the equilibrium symbols accounts for the exchange processes shown in Fig. 4.



The other novel species is formulated as the dimeric adduct between pyridine and the borinic anhydride, $\text{Ar}_2\text{BOBAR}_2(\text{py})$ (**5_{py}** in Scheme 4). This formulation is based on the ^{19}F spectrum (no proton signal attributable to this species was detected). The patterns of resonances (three couples of signals of the same intensity in the three *ortho*, *para*, *meta* regions, see Fig. 2, top trace) cannot arise either by a trimeric or by a monomeric species (taking into account that at room temperature the two aromatic groups on each boron centre are always dynamically equivalent). On the contrary, this pattern agrees with a dimeric structure, in which two couples of aromatic rings are bonded to two different boron atoms. The presence of a tri-coordinated boron centre is revealed by the position of one of the *para* resonances, which lies at very low field (quite close to the signal of **1_m**), with a $\Delta\delta_{m,p}$ of 11.0 ppm at 293 K. Strictly comparable NMR data were previously found for the analogous adduct between borinic anhydride and THF [4], whose nature had been confirmed by the direct reaction between THF and the anhydride. The slight upfield shift observed for **5_{py}** is in line with the higher donor power of pyridine with respect to THF.

The formation of the anhydride implies release of a corresponding amount of water, which at this temperature is bonded to **1_m**, to give the well known $\text{Ar}_2\text{B}(\text{OH})(\text{OH}_2)$ adduct (**2_{H2O}**) [3,4]. Therefore the overall process of formation of **5_{py}** from $\text{Hpy}^+ \cdot \text{3}$

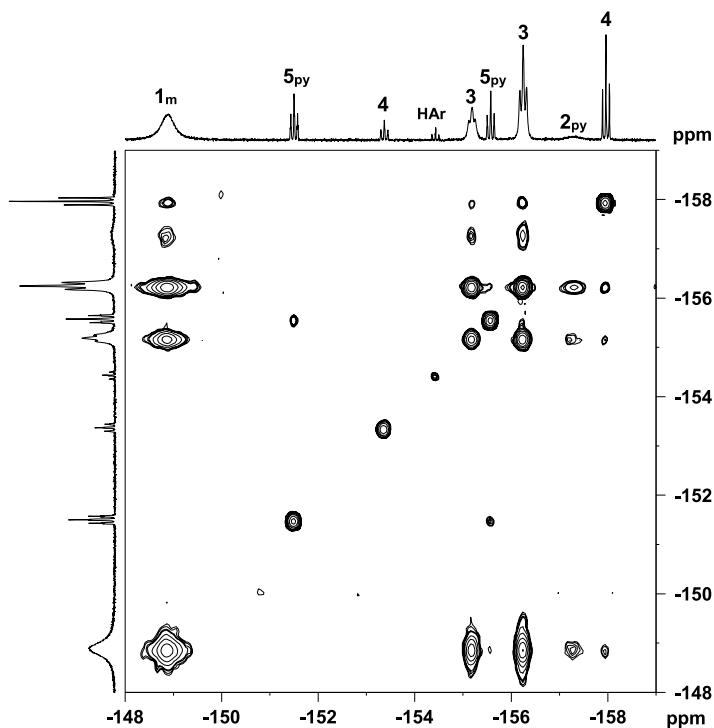
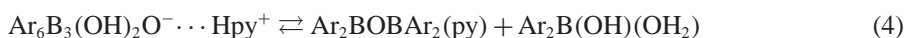


Fig. 4. Para region of a [¹⁹F, ¹⁹F]-EXSY experiment on a sample of **1** treated with ca. 0.33 equiv of py-d₅ (CD₂Cl₂, 293 K, 7.17).

could follow the stoichiometry expressed by Eq. (4).



It is reasonable to assume that the B-bonded water molecule is further stabilized by hydrogen-bonding interactions, either mutual (as for the dimeric form of **2**_{MeOH} depicted in Scheme 1) or with pyridine. In the latter case, proton transfer might take place (equilibrium 5), to give the Hpy⁺Ar₂B(OH)₂⁻ ion pair, due to the Brønsted acidity of a water molecule bonded to a boron atom, as it occurs for the adduct between water and B(C₆F₅)₃ [21].



A detailed analysis of the integration ratios suggest that **2**_{H₂O} does interact with pyridine. However, a deeper insight into the nature of this species was hampered by its low concentration and by the fact that equilibrium 4 is shifted to right only at high temperature, where fast intermolecular exchange processes hinder detection of separated resonances for each species. Indeed, the position and the large bandwidth of the ¹⁹F signals ascribable to the different monomeric forms of **1** (altogether indicated by **1**_m in Fig. 2), indicate that they are averaged by fast exchange between **1**_m and its water

adduct [3]. The ^1H spectrum (Fig. 3) shows a broad resonance at δ 4.4 ppm attributable to the BOH protons of $\mathbf{1}_m$ (including its water adduct) and $\mathbf{2}_{\text{py}}$, which at this temperature are in fast exchange with the protons of water (either free or bonded).

By contrast, the trinuclear anions $\mathbf{3}$ and $\mathbf{4}$ exhibit separated BOH resonances, with respect to such broad averaged resonance (Fig. 3). This can be attributed to the fact that all the BOH protons of $\mathbf{3}$ and $\mathbf{4}$ are buried within a cage of Ar groups and are then involved in strong hydrogen-bond interactions with fluorine atoms. This is supported by a [^1H , ^{19}F]-HOESY experiment, that showed cross peaks between the BOH protons and the *ortho* fluorine atoms (see Fig. S3 in Supporting Information), thus confirming their close proximity. The resonances of the Hpy^+ counterion are instead averaged, at 293 K, either by proton exchange or by fast migration of the cation among the two different anions.

In the case of $\mathbf{4}$, the close interaction between the BOH proton and the surrounding *ortho* fluorine atoms was indicated also by the structure of the ^1H signal (at δ ca. 7.5 ppm), which at 293 K acquired a fine structure (9 lines, J_{HF} 3.3 Hz, as shown in the inset of Fig. 3), attributable to through-space coupling with the eight *ortho* fluorine atoms of the four aromatic rings of the $\text{Ar}_2\text{B}(\text{OH})\text{BAr}_2$ fragment, made equivalent by fast dynamics (as previously observed for $\text{HDMAN}^+\cdot\mathbf{4}$ [6]). This was not observed for the BOH protons of $\mathbf{3}$, because the proton signal is slightly broadened by the exchange processes described in the next paragraph.

Noteworthy, the partial fragmentation of $\mathbf{3}$ was perfectly reversible: on lowering the temperature back to 263 K the adduct $\mathbf{3}$ was quantitatively restored, as shown in Fig. 5.

A ^{11}B NMR spectrum at 293 K (Fig. 6) showed two resonances, one in the region of tetra-coordinated (δ 5.8) and one in the region of tri-coordinated (δ 39.9) boron atoms [1,22–26]. Their intensity ratio well corresponded to the overall ratio (ca. 2 : 3) between the tri-coordinated (mainly $\mathbf{1}_m$, plus the tri-coordinated boron centres in $\mathbf{4}$ and $\mathbf{5}_{\text{py}}$) and tetra-coordinated (all the other ones, including $\mathbf{2}_{\text{H}_2\text{O}}$) species observed in the ^{19}F spectra. In particular, the spectrum confirmed the presence of a large amount of $\mathbf{1}_m$ in the reaction mixture at room temperature, after addition of 0.33 equiv.

3.3 The intra and inter-molecular dynamic processes

The ^{19}F spectra of Fig. 1 (in particular the inset, showing three signals with the same integrated intensity in the *para* region) indicates that in the $\text{Hpy}^+\cdot\mathbf{3}$ ion pair the anion $\mathbf{3}$ has C_2 symmetry, at variance with the C_s symmetry observed for the same anion in the ion pair with a different cation, *i.e.* the $\text{Ar}_2\text{B}(\text{H}_2\text{O})_2^+$ species formed in the mixture $\mathbf{1}/\text{THF}$ [4]. In that case, four signals, in the ratio 2 : 2 : 1 : 1, had been observed in the *para* region. The DFT modelling reported in paragraph 3.1 confirmed the C_2 symmetry of the anion $\mathbf{3}$ paired to Hpy^+ [17]. Therefore, in the limiting ^{19}F spectrum the three couples of nonequivalent aromatic rings of $\mathbf{3}$ should afford fifteen (six *ortho*, three *para*, six *meta*) resonances of the same integrated intensities, as found for instance in the low temperature spectrum of the $\mathbf{1}_t\cdot\text{THF}$ adduct. However, the spectra resulted heavily affected by dynamics.

Two kinds of intramolecular processes can occur in the $\text{Hpy}^+\cdot\mathbf{3}$ ion pair: (*i*) the concerted rotation of each aromatic ring around its B–C bond, which leads to the

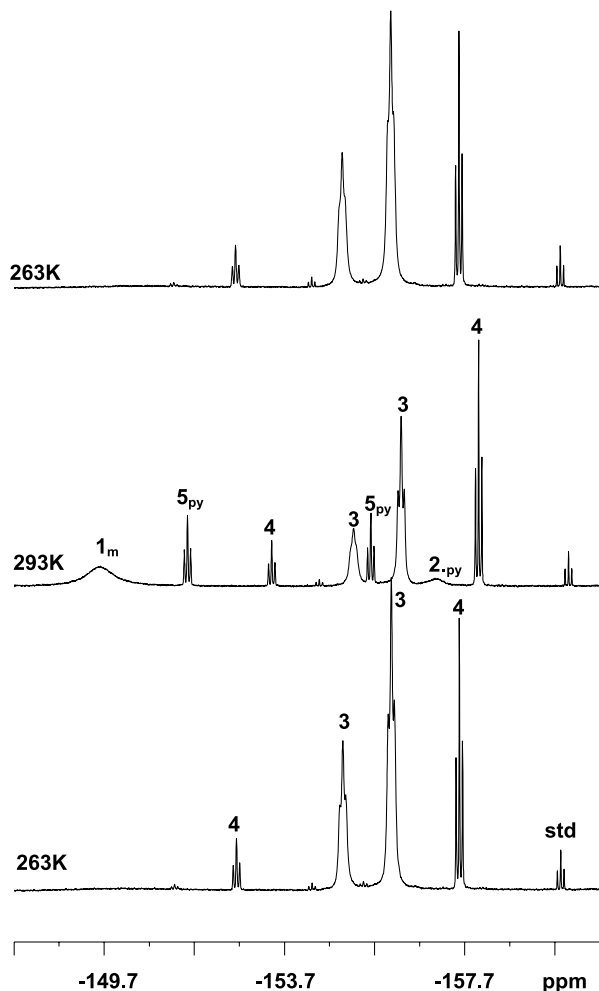


Fig. 5. *Para* region of variable temperature ^{19}F NMR spectra of a sample of **1** treated with *ca.* 0.33 equiv of $py-d_5$ (CD_2Cl_2 , 7.1*T*). The temperature was moved from 263 K (bottom trace) to 293 K (middle trace) and then back to 263 K (top trace), showing the perfect reversibility of the fragmentation of anion **3**.

equalization of the *ortho* and *meta* positions within each ring, and (ii) the flopping of the cycle, consisting in the *pseudo-axial-pseudo-equatorial* interconversion of the two aromatic rings on each of two boron atoms connected by the bridging $O^- \cdots H-py^+$ group. At a temperature as low as 178 K both these processes were still active on the NMR time scale, giving rise to very broad and unresolved resonances, particularly in the *ortho* and *meta* regions, as shown in Fig. 1. The limiting spectrum was attained only by using over-frozen samples (at 170 K), as shown in Fig. 7. A ΔG^\ddagger value of *ca.* 32 kJ mol^{-1} at 176 K was estimated for process *ii*, by the coalescence temperature of the two resonances at higher field in the *para* region, not affected by process *i*.

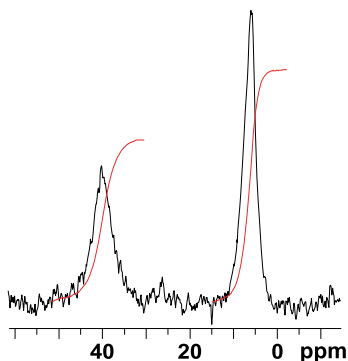


Fig. 6. ^{11}B NMR spectrum on a sample of **1** treated with *ca.* 0.33 equiv of py-d_5 (CD_2Cl_2 , 293 K, 7.1T).

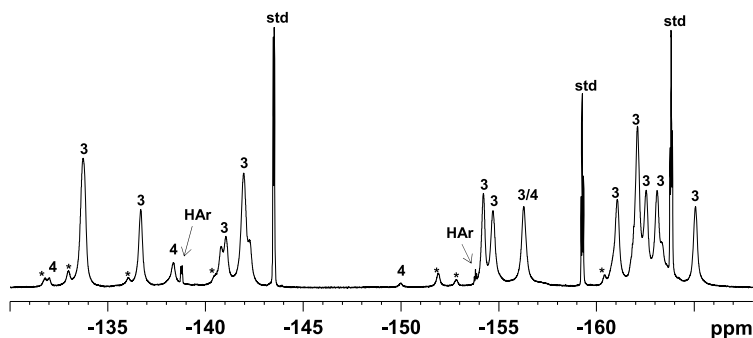


Fig. 7. ^{19}F NMR spectrum of **1** treated with *ca.* 0.33 equiv of py-d_5 (CD_2Cl_2 , 170 K, 9.4T). The asterisk marks the detectable separated resonances of $\mathbf{1}\cdot\text{H}_2\text{O}$ [27].

On raising the temperature, the increase of the rate of both the processes creates an apparent mirror, raising the symmetry of the ion pair from C_2 to C_{2v} . Accordingly, at temperatures higher than 220 K the resonances in the *ortho* and in the *para* regions progressively resolved into two signals in the ratio 2 : 1, while accidental overlap occurred in the *meta* region, as shown in the variable temperature spectra of Fig. 2.

At higher temperatures a third dynamic process became active on the NMR time scale. A $^{19}\text{F}, ^{19}\text{F}$ -EXSY experiment at 256 K showed exchange cross-peaks between the two signals of **3** in each of the *ortho*, *para* and *meta* regions (Fig. S4 in Supporting Information), implying exchange between the singular boron atom and the two boron atoms bridged by the negatively charged oxygen atom. Such exchange cannot be intramolecular, but rather it must go *via* bimolecular (either associative or dissociative) mechanisms. This process results also in the exchange between the pyridinium proton and the two BOH protons of $\text{Hpy}^+\cdot\mathbf{3}$ and accounts for the broadening of their resonances observed at the higher temperatures.

The dynamic behavior of $\text{Hpy}^+\cdot\mathbf{3}$ shows significant differences with respect to what observed for the neutral $\mathbf{1}\cdot\text{THF}$ adduct [4]. In the latter cases both processes *i* (the rotation of the aromatic rings around the B–C bonds) and *ii* (the flopping of the cycle

conformation) were much more hindered than in the present case, so that the limiting spectrum appeared at higher temperatures (at 183 K it was possible to observe fifteen sharp resonances with a clearly detectable fine structure). In particular the kinetic constant estimated for the process of cycle flopping in the neutral $1_t \cdot THF$ adduct was as low as 0.9 s^{-1} at 183 K, whereas the ΔG^\ddagger value estimated for $Hpy^+ \cdot 3$ at 176 K corresponds to a much larger kinetic constant value ($> 10^3 \text{ s}^{-1}$). Most likely the decreased rigidity of anion **3**, with respect to neutral $1_t \cdot THF$, is due to lack of one of the OH protons, which relieves two aromatic rings from the constraints arising from hydrogen-bonding with this hydrogen atom. In agreement with this, the cycle flopping of anion **3** in the $HDMAN^+ \cdot 3$ ion pair was even faster than in $Hpy^+ \cdot 3$, due to the weak cation-anion interaction, and only two ^{19}F signals in the ratio 2 : 1 were present at a temperature as low as 173 K [6].

By contrast, in the neutral $1_t \cdot THF$ adduct, the equalization of the three boron centres was much faster than in anion **3**, because it required only migration of THF among the three BOH groups, whereas in $Hpy^+ \cdot 3$ the equalization requires preliminary back proton transfer (equilibrium 2), followed by pyridine migration. Therefore even at room temperature two signals (ratio 1 : 2) are observed for each of the three regions of the ^{19}F spectrum of $Hpy^+ \cdot 3$, whereas in the case of $1_t \cdot THF$ all the resonances, in each of the three regions, merged in a single averaged signal, starting already from 240 K [4].

On the other hand, the species $Hpy^+ \cdot 4$ shows always two signals in a 1 : 4 ratio, in line with the higher conformational lability expected for an anionic species possessing five aromatic rings only.

A few dynamic processes involving exchange of Ar_2BOH units among different compounds have also been detected, by using $[^{19}F, ^{19}F]$ -EXSY experiments.

The experiment of Fig. S4, at 256 K, showed exchange between $Hpy^+ \cdot 3$ and 1_m . This implies fragmentation/reaggregation of the trimeric unit, which must be catalysed by pyridine, since the equilibrium between 1_m and 1_t is very slow in the absence of a base (see Introduction). The small volume of the cross-peaks indicates that such exchange is very slow, and then it alone cannot be responsible for the above discussed strong correlations between the signals of **3**.

An analogous experiment at 293 K (Fig. 4) showed that at this temperature also the pyridine adduct 2_{py} is involved in the monomer-trimer exchange (most likely due to migration of pyridine among different 1_m molecules). Such exchange is responsible for the large bandwidth of these signals, which makes poorly detectable the species with the lowest concentration (*i.e.* 2_{py}). Fig. 4 shows that even the Ar_2B fragments of the dearylated species **4** are exchanging with 1_m (and then with **3**) at 293 K (although the rate of the exchange is quite low, on the basis of the cross-peaks intensities). By contrast, as expected, 5_{py} is not involved in this intermolecular exchange and Fig. 4 shows only exchange within the species 5_{py} itself, arising from pyridine migration between the two boron centres.

3.4 Addition of 1 equivalent of pyridine

Further pyridine addition (above 0.33 equiv), at low temperature, caused fragmentation of the trimeric oligomers, which were the dominant species in the low temperature re-

action mixtures obtained by addition of 0.33 equiv (as described in the Sect. 3.1). The decrease of the concentration of the oligomers is due to the formation of the covalent Lewis acid-base adduct between **1_m** and pyridine, namely **2_{py}** in Scheme 4. After addition of 1 equiv of pyridine, **2_{py}** was the only boron containing species detectable in solution, either at low or room temperature: three sharp signals were observed in the ¹⁹F spectrum and one resonance in the ¹H spectrum (δ 4.1 ppm) [28]. The latter resonance is significantly upfield shifted with respect to the usual position of the BOH signals in these systems (δ 6–8 ppm): DFT computations reproduced such high field shift. Indeed, the chemical shift predicted by B3LYP-GIAO calculations (see Table S1) for the Lewis acid-base adduct **2_{py}** is 3.92 ppm, to be compared with the value of 7.81 computed for **1_m** (very close to the experimental one, 7.41 ppm [3]). Moreover, the computation further excludes that pyridine interact with **1_m** *via* hydrogen bond, since a value of 14.28 ppm is computed for the hypothetical hydrogen-bonded species **1_m ··· py** (see Table S1). As a further evidence, the small difference between the ¹⁹F chemical shift of the *para* and *meta* fluorine atoms observed experimentally is well reproduced by calculations on the adduct **2_{py}** ($\Delta\delta_{m,p} = 5.4$ ppm), while the value of $\Delta\delta_{m,p} = 12.0$ ppm predicted for **1_m ··· py** is more similar to those computed for species containing trigonally coordinated boron atoms (see Table S1) [29].

The molecular structure of **2_{py}** was confirmed by a single crystal X-ray analysis. The asymmetric unit comprises four **2_{py}** molecules (labeled A to D in Fig. 8), forming a hydrogen-bonded tetramer with a folded square (OH)₄ core, as depicted in Scheme 5. The geometric parameters of the four independent molecules are similar, in particular as far as the coordination of the tetrahedral boron atom is concerned (Table S2). The molecules however significantly differ in the propeller-like conformation of the three six-membered ring bound to the boron center (one pyridine and two pentafluorophenyl ligands), as evidenced by the dihedral angles around the B–N and B–C bonds. The supramolecular tetramer is held together by four O–H ··· O hydrogen bonds and by face-to-face π -stacking interactions involving couples of pentafluorophenyl ligands bound to adjacent boron atoms (Fig. 8). All these structural features have been previously observed in the crystal structure of some bisarylborinic acids [30], which aggregates as hydrogen-bonded tetramers composed of trigonally (instead of tetrahedrally) coordinated boron species. The four pyridine ligands form (less tight) π -stacking interactions, as can be seen in Fig. 8. The ¹⁹F NMR data, measured by dissolving selected crystals in CD₂Cl₂ at low temperature, were in good agreement with those measured in the reaction mixtures containing 1 equiv of pyridine.

The disappearance of **3** upon addition of an amount of base exceeding 0.33 equiv was previously observed in the titrations of **1** with DMAN. In that case, however, the reaction product was the trimeric dearylated species **4**, whereas in the present case fragmentation of the trimer is the main process, as described above. Such different reactivity can be explained taking into account that DMAN cannot behave as Lewis base, so starting into the cascade of events responsible for the fragmentation observed in the case of pyridine [31].

Noteworthy, the ¹⁹F signals of the ion pair Hpy⁺ · **4** in the spectra recorded at intermediate titration steps (for instance 0.66 equiv) were strongly upfield shifted with respect to those observed in the spectra at 0.33 equiv, and were almost identical to those observed for the ion pair HDMAN⁺ · **4**. This can be explained by assuming that a frac-

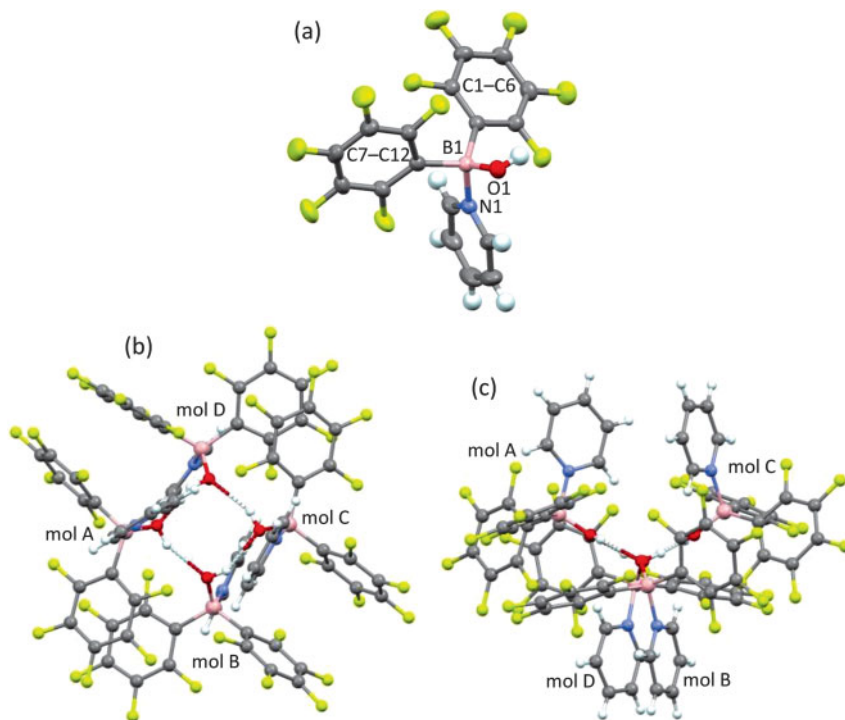
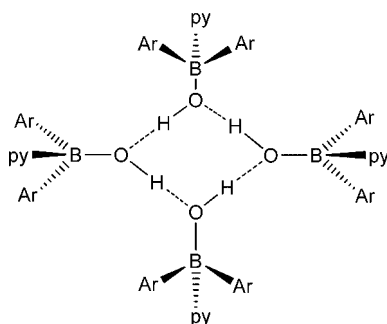


Fig. 8. (a) Ellipsoid plot of one of the four independent molecules found in the crystal structure of 2_{py} (molecule A) showing a partial labeling scheme. Top (b) and frontal (c) view of the hydrogen-bonded tetramer showing the labeling of the molecules.



Scheme 5. The supramolecular aggregation of 2_{py} observed in the crystal structure.

tion of pyridine interacts with the pyridinium cation, to give the homoconjugated pair $py \cdots H \cdots py^+$. This interaction breaks the hydrogen bond with the oxygen atom of **4** and leads to a loose ion pair, similar to that formed with $HDMAN^+ \cdot 4$. In agreement with this, the separation between the *para* and *meta* resonances of the trivalent boron atom of **4** decreased from 10.8 to 8.9 ppm, on increasing the amount of pyridine from 0.33

to 0.66 equiv. It has been previously remarked that the delocalization of the negative charge in tight ion pairs shifts downfield the ^{19}F *para* resonance [1,32].

This effect could not be observed for anion **3**, due to its broad signals and its fast disappearance upon pyridine addition.

4. Conclusions

The data presented in this work provided additional insights into the not trivial behaviour of the chameleonic compound bis(pentafluorophenyl)borinic acid (**1**) in the presence of different oxygen and nitrogen bases.

Pyridine is a stronger Lewis base than THF [33], when we consider its propensity to form dative bonds with an archetypal Lewis acid such as BF_3 in CH_2Cl_2 . Along the same line, it can be reasonably considered also stronger than methanol and water, since the gas phase affinity of the latter two bases for BF_3 is lower than that of THF [34].

On the other hand, pyridine is also a better hydrogen-bond acceptor than the other three bases: according to the $\text{p}K_{\text{BHX}}$ scale, which measures the equilibrium constants of the association with 4-fluorophenol, the following values have been reported: pyridine 1.86, THF 1.28, methanol 0.82, water 0.65 [35]. The same order is found in the β_2 scale: pyridine 0.62, THF 0.51, methanol 0.41, water 0.38 [36].

Moreover, pyridine is a much stronger Brønsted base than the other three Lewis bases. *A priori* it is therefore impossible to establish if Lewis acid-base interactions or hydrogen bonds or proton transfer processes would play the dominant role in the speciation of **1**, at different temperatures in the presence of different amounts of pyridine.

The experimental results have shown that the reaction of **1** with 1 equiv of pyridine affords quantitatively the Lewis acid-base adduct $\text{Ar}_2\text{B}(\text{OH})(\text{py})$ (**2_{py}**). Surprisingly, this is the first time that such apparently trivial result is obtained, since the other three Lewis bases previously investigated had shown a quite different behaviour. This finding suggests that the Lewis basicity of pyridine plays here the dominant role in defining the nature of the species. DFT computations have confirmed the higher stability of the adduct **2_{py}** with respect to $\mathbf{1}_m \cdots \text{py}$. However, at least in the solid state, also hydrogen bond interactions are operative, leading to the supramolecular organization of the **2_{py}** adduct in the form of the cyclic tetramer shown in Fig. 8.

On the other hand, when **1** is treated with less than 1 equiv of pyridine, the fast trimerization pathway already observed in the case of other Lewis bases (Scheme 2) becomes operative. The driving force for this process is provided by the Lewis basicity of pyridine (with the consequent increased Lewis basicity of the oxygen atom in the adducts **2_L**, with respect to $\mathbf{1}_m$), but the Brønsted basicity of pyridine determines the nature of the final product, which was shown, by both spectroscopic and computational evidence, to be the ion pair between deprotonated trimer and pyridinium cation ($\text{Hpy}^+ \cdot \mathbf{3}$).

On raising the temperature the trimer underwent entropy-driven fragmentation, while upon addition of pyridine enthalpy-driven fragmentation was observed. In the latter case, the Lewis-acidic Ar_2BOH units, which in the trimeric oligomer were engaged in mutual Lewis acid-base $\text{Ar}_2(\text{OH})\text{B}-\text{O}(\text{H})\text{BAr}_2$ interactions, were progressively cap-

tured by pyridine, which is a stronger Lewis base than **1**, to give the covalent Lewis acid-base adduct **2_{py}**.

The behaviour of pyridine showed also many significant differences with respect to that of the stronger Brønsted base DMAN (p*K*_a 12.1 vs. 5.25 for pyridine, in water). First, the interaction of **1_m** with DMAN afforded the anion Ar₂BO⁻, responsible for the anionic route followed in the trimerization pathway in that case. With pyridine, on the contrary, the neutral adduct **2_{py}** is initially formed, which is responsible for the 'neutral' trimerization pathway observed in this case. Moreover, the pyridinium cation is able to establish a strong hydrogen bond with the deprotonated trimer (resulting in the tight Hpy⁺·**3** ion-pair), which was not possible for the HDMAN⁺ cation, resulting in a much looser interaction between anion **3** and HDMAN⁺ cation. ¹⁹F chemical shifts proved to be a reliable probe of the nature of the ion pair [1]. A further difference with respect to DMAN is provided by the marginal role here played by dearylated species: pyridine is not a Brønsted base strong enough to efficiently promote the dearylation process.

Worth of mention is also the reversible formation of the adduct between pyridine and the anhydride of borinic acid. The partial dehydration of **1** to its anhydride had been previously observed at low temperature [3], and it was driven by the stabilization of the released water molecule in a cycle in which it was simultaneously covalently bonded to a boron atom and hydrogen-bonded to an oxygen atom (see the species **1_t**·H₂O_{endo} in Scheme 1). Here the formation of the anhydride occurs at high temperature, but the driving force is analogous, *i.e.* the two-fold stabilization of the water molecule in the Ar₂B(OH)OH₂·...py adduct, which most likely evolves to give the Ar₂B(OH)₂⁻·...Hpy⁺ ion pair.

In conclusion the work here described confirms that the speciation of **1** in the presence of bases is not straightforwardly predicable, but can be rationalized by the subtle balance among Lewis and Brønsted acidity-basicity as well as hydrogen bond donor-acceptor capability of the two reagents.

References

1. T. Beringhelli, D. Donghi, D. Maggioni, and G. D'Alfonso, *Coordin. Chem. Rev.* **252** (2008) 2292.
2. T. Beringhelli, G. D'Alfonso, D. Donghi, D. Maggioni, P. Mercandelli, and A. Sironi, *Organometallics* **22** (2003) 1588.
3. T. Beringhelli, G. D'Alfonso, D. Donghi, D. Maggioni, P. Mercandelli, and A. Sironi, *Organometallics* **23** (2004) 5493.
4. T. Beringhelli, G. D'Alfonso, D. Donghi, D. Maggioni, P. Mercandelli, and A. Sironi, *Organometallics* **26** (2007) 2088.
5. D. Donghi, D. Maggioni, T. Beringhelli, G. D'Alfonso, P. Mercandelli, and A. Sironi, *Eur. J. Inorg. Chem.* (2008) 1645.
6. D. Donghi, D. Maggioni, T. Beringhelli, and G. D'Alfonso, *Eur. J. Inorg. Chem.* (2008) 3606.
7. G. J. P. Britovsek, J. Ugolotti, P. Hunt, and A. J. P. White, *Chem. Commun.* (2006) 1295.
8. See for example (a) K. Ishihara, and H. Yamamoto, *Eur. J. Org. Chem.* (1999) 527; (b) K. Ishihara, H. Kurihara, and H. Yamamoto, *J. Org. Chem.* **62** (1997) 5664; (c) K. Ishihara, H. Kurihara, and H. Yamamoto, *Synlett* (1997) 597.
9. Recent patents dealing with the synthesis or use of bis(pentafluorophenyl)borinic acid include (a) T. Sell, J. Schottek, N. S. Paczkowski, and A. Winter, Patent WO 2006124231 (2006) to Novolen Technology, (b) T. Neumann, S. Herrwerth, T. Reibold, and H.-G. Krohm, Patent DE

- 102005004676 (2005) to Goldschmidt G.m.b.H., (c) R. Kratzer, Patent WO 04041871 (2004) to Basell Polyolefins, (d) R. Kratzer, Patent WO 04007570 (2004) to Basell Polyolefins, (e) R. Kratzer and V. Fraaije, Patent WO 04007569 (2004) to Basell Polyolefins, (f) K. Takei, K. Mizuta, K. Aoki, and K. Takebe, Patent JP 2004265785 (2004) to Nippon Shokubai.
10. A. L. Van Geet, *Anal. Chem.* **42** (1970) 679.
 11. A. D. Becke, *J. Chem. Phys.* **98** (1993) 5648.
 12. J. Tomasi, B. Mennucci, and R. Cammi, *Chem. Rev.* **105** (2005) 2999.
 13. J. R. Cheeseman, G. W. Trucks, T. A. Keith, and M. J. Frisch, *J. Chem. Phys.* **104** (1996) 5497.
 14. (a) H. Fukaya and T. Ono, *J. Comput. Chem.* **25** (2004) 51, (b) R. Jain, T. Bally, and P. R. Rablen, *J. Org. Chem.* **74** (2009) 4017.
 15. Gaussian 09 (revision C.01), Gaussian Inc., Wallingford, CT (2010).
 16. See for example N.S. Golubev, G. S. Denisov, S. N. Smirnov, D. N. Shchepkin, and H.-H. Limbach, *Z. Phys. Chem.* **196** (1996) 73 and references therein.
 17. For the isolated anion **3** we previously found a C_s structure to be more stable than a corresponding C_2 one [4]. However, in $\text{Hpy}^+\cdot\mathbf{3}$ unfavorable steric interactions between the pentafluorophenyl groups and the pyridinium cation led to a stabilization of the C_2 symmetric conformation, while the corresponding C_s geometry results not to be a minimum. Analogous considerations apply to the neutral species $\mathbf{1}_t\cdot\text{py}$.
 18. In the case of the reaction with DMAN, the formation of dearylated anion **4** was accompanied by the formation of a corresponding amount of pentafluorobenzene [6]. In the present case the detected amount of pentafluorobenzene seems to be smaller than expected, accounting only for the 50–60% of the anion **4** formed, although the much smaller percentage of **4** formed in the reaction with pyridine and the presence of many very broad ^{19}F resonances hamper an accurate evaluation of the integration ratios. Most likely the formation of $\text{Hpy}^+\cdot\mathbf{4}$ involved, in part, the very little amount of $\text{ArB}(\text{OH})_2$ which always contaminates samples of Ar_2BOH , due to slow hydrolysis by traces of water, and which is hardly detectable by NMR for its small solubility in CD_2Cl_2 .
 19. See for example (a) L. Sobczyk, B. Czarnik-Matusiewicz, M. Rospenk, and M. Obrzud, *Journal of Atomic, Molecular, and Optical Physics* (2012), 217932, (b) V. Schreiber, A. Kulbida, M. Rospenk, L. Sobczyk, A. Rabold, and G. Zundel, *J. Chem. Soc. Faraday T.* **92** (1996) 2555.
 20. S. Grundemann, S. Ulrich, H.-H. Limbach, N. S. Golubev, G. S. Denisov, L. M. Epstein, S. Sabo-Etienne, and B. Chaudret, *Inorg. Chem.* **38** (1999) 2550.
 21. (a) T. Berighelli, D. Maggioni, and G. D'Alfonso *Organometallics* **20** (2001) 4927, (b) C. Bergquist, B. M. Bridgewater, C. J. Harlan, J. R. Norton, R. A. Friesner, and G. Parkin, *J. Am. Chem. Soc.* **122** (2000) 10581.
 22. R. G. Kidd, Boron-11, in: *NMR of Newly Accessible Nuclei*, Vol. 2, Chapt. 3, P. Laszlo (Ed.), Academic Press, New York (1983), pp. 49–77.
 23. ^{11}B chemical shifts for neutral tetrahedral boron derivatives bearing pentafluorophenyl substituents are normally found between -20 and $+20$ ppm [24,25], whereas tri-coordinated boron derivatives show typically ^{11}B chemical shift in the range 32.5–74.9 ppm [24,26].
 24. See for example (a) D. J. Parks, W. E. Piers, and G. P. A. Yap, *Organometallics* **17** (1998) 5492, (b) W. Fraenk, T. M. Klapotke, B. Krumm, and P. Mayer, *Chem. Commun.* (2000) 667, (c) G. Kehr, R. Fröhlich, B. Wibbeling, and G. Erker, *Chem.-Eur. J.* **6** (2000) 258.
 25. See for example (a) Y. Sun, W. Piers, and J. R. Rettig, *Organometallics* **15** (1996) 4110, (b) D. J. Parks, W. E. Piers, M. Parvez, R. Atencio, and M. J. Zaworotko, *Organometallics* **17** (1998) 1369, (c) H. Jacobsen, H. Berke, S. Döring, G. Kehr, G. Erker, R. Fröhlich, and O. Meyer, *Organometallics* **18** (1999) 1724.
 26. See for example (a) D. Vagedes, R. Fröhlich, and G. Erker, *Angew. Chem. Int. Edit.* **38** (1999) 3362, (b) L. H. Doerr and M. L. H. Green, *J. Chem. Soc. Dalton Trans.* (1999) 4325, (c) S. Dagorne, I. A. Guzei, M. P. Coles, and R. F. Jordan, *J. Am. Chem. Soc.* **122** (2000) 274.
 27. Unpublished results.
 28. The positions of the ^{19}F and ^1H signals of $\mathbf{2}_{\text{pp}}$ at intermediate titration stages were downfield shifted with respect to those above reported, due to fast exchange with some $\mathbf{1}_{\text{m}}$ still present in solution before the attainment of the stoichiometric ratio (see for instance the analogous progressive upfield shift of the resonances of $\mathbf{1}_{\text{m}}$ upon stepwise addition of water [3]).

29. A direct comparison between experimental and computed ¹⁹F chemical shift values can be misleading. Indeed, the excellent agreement between the chemical shift experimentally observed for the *ortho* and *para* fluorine atoms of the **2_{py}** adduct and those computed for **1_m**·**py** is fortuitous, since the computed ¹⁹F chemical shift are systematically high field shifted by 2–6 ppm (see the entries for **1_m** and **1_t** in Table S1 in Supporting Information).
30. (a) K. J. Weese, R. A. Bartlett, B. D. Murray, M. M. Olmstead, and P. P. Power, *Inorg. Chem.* **26** (1987) 2409, (b) C. D. Entwistle, A. S. Batsanov, and T. B. Marder, *Acta Crystallogr.* **E63** (2007) o2639.
31. The disappearance, at the end of the titration, of signals attributable to species arising from the monoarylated boron fragment of **4** (which cannot transform into **2_{py}**) can be explained by formation of insoluble boronic acid ArB(OH)₂, by the adventitious water present in solution.
32. A. D. Horton and J. de With, *Organometallics* **16** (1997) 5424.
33. P.-C. Maria and J.-F. Gal, *J. Phys. Chem.* **89** (1985) 1296.
34. A. Rauk, I. R. Hunt, and B. A. Keay, *J. Org. Chem.* **59** (1994) 6808.
35. C. Laurence, K. A. Brameld, J. Graton, J.-Y. Le Questel, and E. Renault, *J. Med. Chem.* **52** (2009) 4073.
36. M. H. Abraham, P. L. Grellier, D. V. Prior, J. J. Morris, and P. J. Taylor, *J. Chem. Soc. Perk. T.* **2** (1990) 521.